

# Self-Oscillation Multicarrier Light Source Based on Recirculating Frequency Shift Loop

Long Zhang , Zhaoying Wang , Quan Yuan , Jinxin Jiang, Lai Wen, Lipai Song, and Chunfeng Ge 

**Abstract**—A novel scheme of self-oscillation multicarrier light source based on recirculating frequency shift loop (RFSL) is proposed and experimentally demonstrated in this paper. Compared with conventional RFSL-based multicarrier generation schemes, the radio frequency (RF) signal for driving the modulator in RFSL is generated by an internal self-oscillation of the optical carrier instead of the external commercial RF source device. The self-oscillation method significantly reduces the cost of the light source and decreases the phase noise of RF signal and multicarrier signal. In the experiment, we successfully generate a single-mode oscillation RF signal with the phase noise of  $-85.10$  dBc/Hz at 10 kHz offset frequency. A total of 49 multicarrier optical signals from 1550.59 nm to 1554.44 nm with the power fluctuation as low as 3 dB are obtained. The frequency interval is approximately 10.014 GHz, which is equal to the oscillation frequency of the RF signal.

**Index Terms**—Multicarrier light source, recirculating frequency shift loop, self-oscillation, phase noise.

## I. INTRODUCTION

THE generation and the application of multicarrier light source have attracted attentions within recent years [1]–[3]. Because of the advantages of precise frequency interval and uniform power spectrum, multicarrier light source has been widely used in many areas, such as optical arbitrary waveform generation [4], microwave photonics [5], dense wavelength-division multiplexing (DWDM) [6], orthogonal frequency division multiplexing (OFDM) in optical communication system [7] and optical frequency reference for either measurement or optical signal processing [8], [9]. Different schemes have been proposed to generate multicarrier and experimentally demonstrated. In

general, multicarrier generation by intracavity modulation such as mode-locked lasers [10] and optical fiber nonlinearity [11] has poor frequency stability and tunability. In contrast, the external modulation scheme with electro-optic modulator (EOM) driven by RF signal greatly improves the frequency stability without changing the structure of laser cavity. Moreover, the frequency interval of multicarrier is equal to the frequency of the driven RF signal, so it can be tuned flexibly. External modulation, such as cascaded EOMs [12] and EOM driven by optoelectronic oscillator [13], [14], can generate multicarrier through only one optical modulation of seed light, but the number of subcarriers depends on the power of RF signal. Then the external modulation based on recirculating frequency shift loop (RFSL) was proposed [15], [16]. In RFSL, the EOM operating in single-sideband (SSB) mode is used as a frequency shifter to modulate the optical carrier passing through it and a new subcarrier is generated after every roundtrip. Therefore, the number of subcarriers is determined by the number of cycles the optical carrier passing through in RFSL, which reduces the dependence on RF signal power. However, with the increase of the cycle number, noises consisting of intensity noise and phase noise gradually accumulate and therefore deteriorate the quality of multicarrier optical signal. In recent years, the intensity noise of RFSL output multicarrier has been effectively suppressed by optimizing the laser structure [17]. However, there are few reports on how to reduce the multicarrier phase noise of RFSL output. This is because the phase noise of multicarrier output from RFSL is mainly induced by the RF signal driving the EOM [18] and the RF signal is generally provided by an external commercial RF source. Optimizing the phase noise of RF source in high frequency band ( $>10$  GHz) undoubtedly increase the complexity, volume and cost of the system.

In this paper, we propose and experimentally demonstrate a novel scheme of self-oscillation multicarrier light source. Different from the conventional RFSL-based multicarrier generation scheme, the most prominent feature of our scheme is that the RF signal driving the EOM is generated by an optical-electrical-optical self-oscillation loop instead of external commercial RF source. In the process of self-oscillation, the output optical signal of RFSL is converted into electrical signal by a balanced photodetector (BPD) and the electrical signal that is selected and amplified in the electrical domain is fed back to drive the EOM to generate optical signal. By repeating this process, the RF signal gradually acquires the center frequency of the electrical filter and approaches the oscillation condition. Accordingly, the multicarrier optical signal modulated by the optimized RF signal will also form an advantage of oscillation.

Manuscript received May 8, 2021; revised July 1, 2021; accepted July 11, 2021. Date of publication July 14, 2021; date of current version July 29, 2021. This work was supported in part by the National Natural Science Foundation of China under Grants 61275084 and 61605092 and in part by the Natural Science Foundation of Tianjin under Grant 18JCYBJC16800. (Corresponding author: Zhaoying Wang.)

Long Zhang, Zhaoying Wang, Jinxin Jiang, Lai Wen, and Chunfeng Ge are with the Key Laboratory of the Ministry of Education on Optoelectronic Information Technology, School of Precision Instrument and Optoelectronics Engineering, Tianjin University, Tianjin 300072, China (e-mail: longz175@tju.edu.cn; wangzy@tju.edu.cn; jiangjx@tju.edu.cn; wenlai@tju.edu.cn; gechunfeng@tju.edu.cn).

Quan Yuan is with the Key Laboratory of the Ministry of Education on Optoelectronic Information Technology, School of Precision Instrument and Optoelectronics Engineering, Tianjin University, Tianjin 300072, China, and also with the College of Tianjin Renai, 301636 Tianjin, China (e-mail: ewanyuan@tju.edu.cn).

Lipei Song is with the College of Modern Optics, Nankai University, Tianjin 300350, China (e-mail: gm\_imo@nankai.edu.cn).

Digital Object Identifier 10.1109/JPHOT.2021.3097063

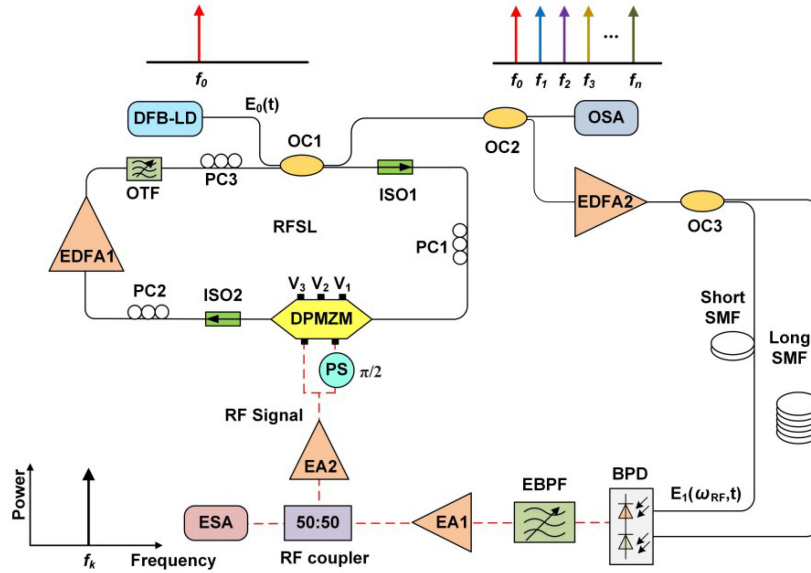


Fig. 1. The diagram of self-oscillation multicarrier light source. DFB-LD: distributed feedback diode laser; OC: optical coupler; ISO: isolator; PC: polarization controller; DPMZM: dual-parallel Mach-Zehnder modulator; PS: phase shifter; EDFA: erbium-doped fiber amplifier; OTF: optical tunable filter; OSA: optical spectrum analyzer; SMF: single mode fiber; BPD: balanced photodetector; EBPF: electrical band pass filter; EA: electrical amplifier; RF coupler: radio frequency coupler; ESA: electrical spectrum analyzer.

Then stable self-oscillation multicarrier with frequency interval equal to the RF signal frequency is output. In the experiment, a single-mode oscillation RF signal is successfully generated with the center frequency at 10.014 GHz. The phase noise of the RF signal is  $-85.10$  dBc/Hz at 10 kHz offset frequency. Meanwhile, the multicarrier optical signal ranging from 1550.59 nm to 1554.44 nm with the power fluctuation of 3 dB is also successfully obtained. The subcarriers number is 49 and the frequency interval between adjacent subcarriers is approximately equal to the RF signal frequency.

## II. PRINCIPLES AND EXPERIMENTAL SETUP

Fig. 1 is the diagram of the self-oscillation multicarrier light source based on recirculating frequency shift loop (RFSL). The distributed feedback diode laser (DFB-LD) outputs single frequency ( $f_0$ ) seed light as the starting frequency of the generated multicarrier. The seed light passes through the optical coupler (OC1), after which 50% of the light is the output of RFSL and the other 50% enters the RFSL. In the RFSL, the seed light enters the dual-parallel Mach-Zehnder modulator (DPMZM) after passing through an isolator (ISO) and a polarization controller (PC). Through controlling the bias voltage, the DPMZM can work on the single-sideband (SSB) mode as a frequency shifter. The optical signal generated by the frequency shift is coupled with the continuous seed light at OC1 and 50% of the output enters the RFSL again. In this case, the optical carrier is added a new subcarrier component after each recirculating process in the RFSL and the frequency interval between two adjacent subcarriers is equal to the frequency of the driven RF signal applied on the DPMZM. The erbium-doped fiber amplifier (EDFA1) in the RFSL is to compensate the optical loss. The optical tunable filter (OTF) is to control the number of subcarriers by adjusting its bandwidth.

Before the self-oscillation is established, the DPMZM is initially driven by electrical signals converted from the light. The electrical signals can be considered as a superposition of sine or cosine waves with random frequencies, phases and amplitudes. Therefore, the frequency shift of the optical carrier modulated by the DPMZM is random and uncertain. The output optical signals of RFSL with different frequency interval are converted into electrical signals with different frequencies by a balanced photodetector (BPD). The electrical signals with frequencies within the bandwidth of the electrical band pass filter (EBPF) are amplified by the electrical amplifier (EA). The electrical signals are fed back into the DPMZM through the RF coupler to repeat the above process. However, in the process of the cycle, only the electrical signal that satisfies the oscillation condition will be kept and gradually establish stable oscillation, but the others will be annihilated.

In order to further analyze the process of self-oscillation and derive the oscillation condition, a frequency component randomly chosen from the electrical signals as the RF signal to drive the DPMZM:

$$V_{in}(\omega_{RF}, t) = V_0 \exp(i\omega_{RF}t) \quad (1)$$

where  $V_0$  and  $\omega_{RF}$  are the amplitude and angular frequency of the RF signal respectively. The seed light from DFB-LD can be expressed as:

$$E_0(t) = \sqrt{2}E_0 \exp(i\omega_0 t) \quad (2)$$

where  $\sqrt{2}E_0$  and  $\omega_0$  are the amplitude and angular frequency of the seed light respectively. The DPMZM generates a new subcarrier component with the angular frequency of  $\omega_0 + \omega_{RF}$  after single SSB modulation on the seed light [19]. Therefore, the output optical signal from RFSL after one round trip contains the seed light and the new subcarrier component. Then after optical amplification by the EDFA2 and the time delay in the SMF, the

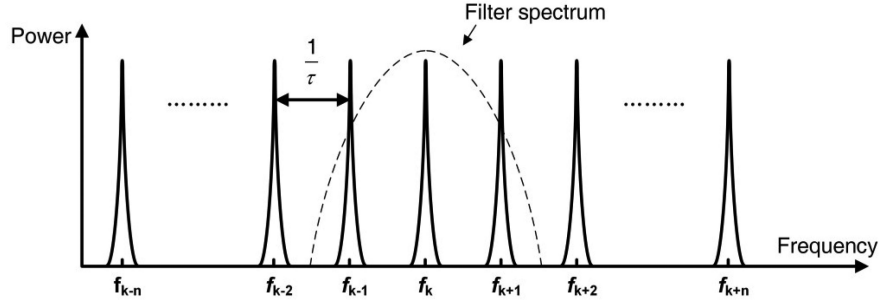


Fig. 2. The Schematic diagram of multimode oscillation RF signal and filter spectrum.

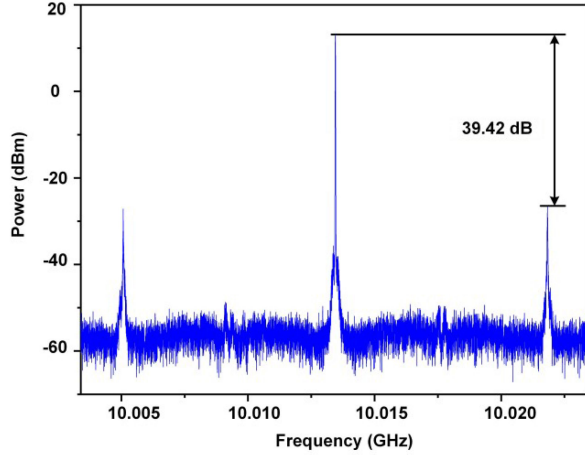


Fig. 3. The RF signal spectrum generated by self-oscillation.

optical signal  $E_1(\omega_{RF}, t)$  can be written as:

$$E_1(\omega_{RF}, t) = G_0 L_0 E_0 \exp(i\omega_0 t) + G_1 L_1 E_0 J_1(m) \times \exp[i(\omega_0 t + \omega_{RF} t + \theta)] \quad (3)$$

where  $J_1(m)$  is the first-order coefficient of the Bessel function expansion,  $m = \pi V_0 / V_\pi$  is the modulation coefficient and  $V_\pi$  is the half-wave voltage of the modulator;  $G_0$ ,  $L_0$  and  $G_1$ ,  $L_1$  are the total optical gain and the loss of the seed light and the subcarrier respectively;  $\theta$  is the phase difference between adjacent subcarriers introduced by the optical path length  $L$  of the oscillation loop.  $L$  includes the loop length of RFSL and the optical path length from OC1 to BPD.  $E_1(\omega_{RF}, t)$  can be detected by the BPD and is converted into electrical signal  $V_{BPD}(\omega_{RF}, t)$  expressed as:

$$V_{BPD}(\omega_{RF}, t) = A E_1(\omega_{RF}, t) \cdot E_1^*(\omega_{RF}, t) \approx A E_0^2 G_0 L_0 G_1 L_1 J_1^2(m) \exp[i(\omega_{RF} t + \theta)] \quad (4)$$

where  $A$  is determined by the responsivity and the load impedance of the BPD. After passing through the EBPf and the EA, the electrical signal becomes:

$$V_{out(1)}(\omega_{RF}, t) = F(\omega_{RF}) G_A L_A \cdot A E_0^2 G_0 L_0 G_1 L_1 J_1^2(m) \times \exp[i(\omega_{RF} t + \theta)] = F(\omega_{RF}) G_{eff} V_{in}(\omega_{RF}, t) \exp(i\theta) = F(\omega_{RF}) G_{eff} \cdot V_{in}(\omega_{RF}, t - \tau) \quad (5)$$

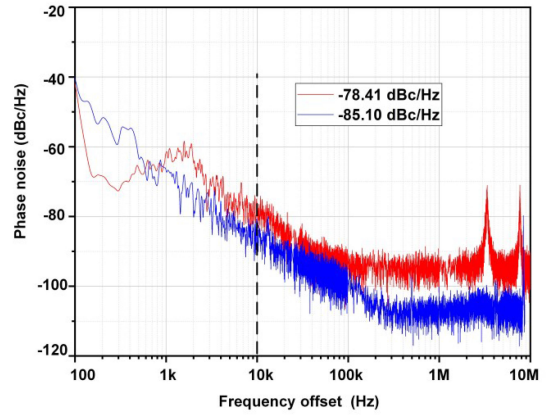


Fig. 4. Phase noise spectra of the RF signals at 10.014 GHz generated by (red) RF source and (blue) self-oscillation.

where  $F(\omega_{RF})$  is the normalized transmission function of the EBPf.  $G_A$  is the signal gain of the EA and  $L_A$  is the signal loss in the electrical domain.  $\tau$  is the total time delay in the time domain corresponding to the total phase  $\theta$ .  $V_{out(1)}(\omega_{RF}, t)$  continues to drive DPMZM as an input electrical signal. After the electrical signal circulates  $n$  cycles in the oscillation loop, the cyclic relationship can be derived from (5) as:

$$V_{out(n)}(\omega_{RF}, t) = F(\omega_{RF}) G_{eff} \cdot V_{out(n-1)}(\omega_{RF}, t - \tau) \quad (6)$$

Accordingly, after several cycles of RFSL, the RF signal becomes the sum of beat signals generated between all light fields output by RFSL. When the open-loop gain  $G_{eff}$  is less than unit, the RF signal can be expressed as [20]:

$$V(\omega_{RF}, t) = \sum_{n=0}^{\infty} V_{out(n)}(\omega_{RF}, t) = \sum_{n=0}^{\infty} F(\omega_{RF}) G_{eff} \exp[i(\omega_{RF} t - n\omega_{RF} \tau)] = \frac{\exp(i\omega_{RF} t)}{1 - F(\omega_{RF}) G_{eff} \exp(-i\omega_{RF} \tau)} \quad (7)$$

The power of the corresponding RF signal is expressed as:

$$P(\omega_{RF}) \propto \frac{1}{1 + |F(\omega_{RF}) G_{eff}|^2 - 2F(\omega_{RF}) |G_{eff}| \cos(\omega_{RF} \tau)} \quad (8)$$

It can be seen from (8) that the RF signals can oscillate as shown in Fig. 2 only when the angular frequencies satisfy

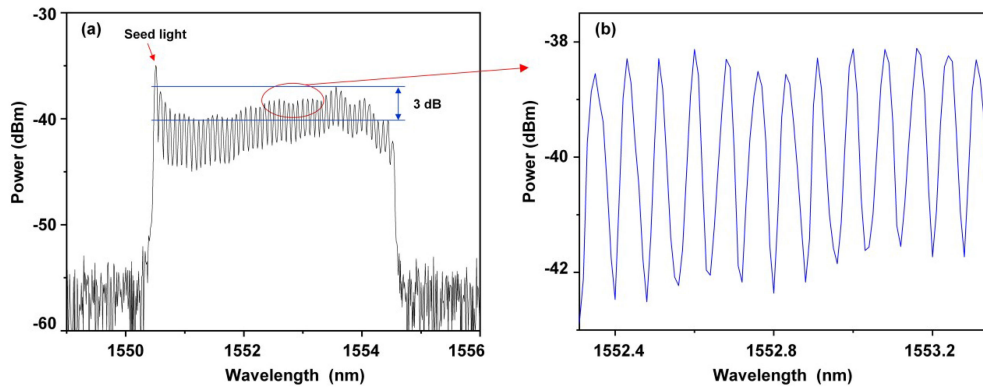


Fig. 5. The optical spectrum of (a) multicarrier optical signal; (b) subcarriers from 1552.35 nm to 1553.31 nm.

$\omega_{RF(k)}\tau = 2\pi f_k\tau = 2k\pi$ . In Fig. 2 the oscillation mode interval is  $f_{k+1} - f_k = 1/\tau$  and  $\tau = nL/c$ , where  $n$  and  $c$  depict the effective refractive index of the fiber and the speed of light velocity in vacuum respectively. In Fig. 1, the EBPF is to filter out undesired modes but output the desired one, which will be gradually optimized and finally has stable oscillation. However, there is a contradiction between mode interval and phase noise in single oscillation loop. Long oscillation loop reduces phase noise but at the same time decreases the mode interval. An EBPF with high quality factor has to be used to sustain single-mode oscillation. To solve this problem, two different lengths of SMFs can be inserted between OC1 and BPD to form a dual oscillation loop structure. Therefore, there are two oscillation loops with different lengths and the mode interval needs to simultaneously meet the two loop lengths. Because of the vernier effect, the mode interval  $1/\tau$  will be ultimately determined by the short oscillation loop. Then the oscillation mode interval is increased significantly. Setting a proper length of the two SMFs and the center frequency of the EBPF will realize the single-mode oscillation of RF signal  $f_k$ . The dual-loop structure suppresses the spurious modes further without the deterioration in phase noise performance [21]. The RF signal  $f_k$  is fed back to drive the DPMZM to generate multicarrier with frequency interval of  $f_k$ . The beat frequency generated by this multicarrier consolidates the oscillation advantage of  $f_k$  again. In this way, after multiple cycles, the photoelectric oscillation loop gradually forms positive feedback and output stable self-oscillation multicarrier with frequency interval of  $f_k$ .

### III. EXPERIMENTAL RESULTS

In order to demonstrate the theoretical analysis, experiments were carried out with the setup shown in Fig. 1. The output of distributed feedback diode laser (DFB-LD) was used as seed light with maximum power of 8 dBm. Its center wavelength was 1550.51 nm and the linewidth was about 500 kHz. The half-wave voltage of the dual-parallel Mach-Zehnder modulator (DPMZM, FUJITSU-FTM7962EP) was 14 V. The long single mode fiber (SMF) was 1 km and the short SMF was 1m. Because there were other optical paths and optical devices in the oscillation loop, the effective lengths of the two oscillation loops were about 1024 m and 24 m respectively. The conversion of optical-to-RF signal was realized by the BPD (0.6 A/W responsivity and 35

GHz bandwidth). Because the maximum optical input power of BPD was 4 dBm, we set the output power of EDFA1 as 14 dBm and EDFA2 to be less than 7 dBm. The central frequency and bandwidth of the EBPF was 10 GHz and 50 MHz respectively. The filtered RF signal was equally divided by the electrical coupler, half of which went into the electrical spectrum analyzer (ESA) and the other half was fed back to drive the DPMZM.

Fig. 3 shows the RF signal spectrum generated by self-oscillation. The spectrum was measured by the ESA (Agilent-N9010A) with the span of 20 MHz and RBW of 10 kHz. The central frequency and the peak power of the RF signal were 10.014 GHz and 12.850 dBm respectively. The side mode suppression ratio was 39.42 dB and the frequency interval between two adjacent oscillation modes was approximately 8.4 MHz, which was consistent with the short oscillation loop length (24 m). It can be believed that the single-mode oscillation RF signal at 10.014 GHz was generated by the self-oscillation. Since the frequency of the RF signal depended on the length of short oscillation loop, its frequency might deviate slightly from the center frequency of the EBPF.

Fig. 4 shows the phase noise spectrums of the RF signals generated by RF source and by self-oscillation. The red line represents the phase noise spectrum of the 10.014 GHz RF signal generated by the commercial RF source (HP83752B) and the phase noise is  $-78.41$  dBc/Hz at 10 kHz offset frequency. The blue line represents the phase noise spectrum of the RF signal that is shown in Fig. 3 and the phase noise is  $-85.10$  dBc/Hz at 10 kHz offset frequency. Because of the presence of local oscillator phase noise of the ESA, the actual phase noise at 10 kHz offset is lower than  $-85.10$  dBc/Hz. The experimental results demonstrate that the RF signal generated by self-oscillation has lower phase noise.

Fig. 5 shows the optical spectrum of the self-oscillation multicarrier optical signal, which was measured by an optical spectrum analyzer (OSA) with a resolution of 0.05 nm. In the experiment, a total of 49 subcarriers, as shown in Fig. 5(a), ranging from 1550.59 nm to 1554.44 nm with the power fluctuation of 3 dB were recorded by setting the optical tunable filter (OTF) bandwidth as 4.12 nm. Fig. 5(b) shows the zoom-in view of the spectrum from 1552.35 nm to 1553.31 nm. There are 13 ultra-flat subcarriers with the power fluctuation lower than 0.42 dB. The fluctuation of multicarrier flatness is due to the uneven gain

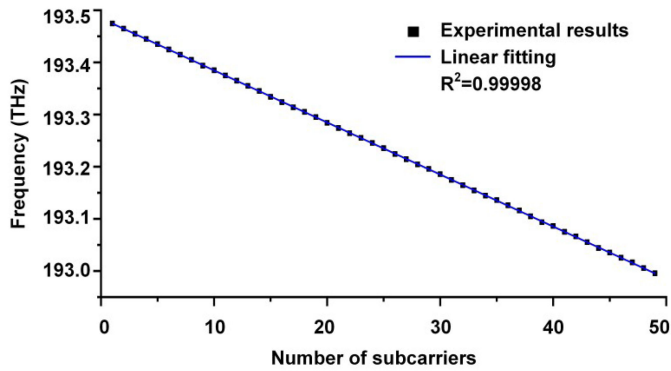


Fig. 6. The frequency of the generated multicarrier optical signal.

spectrum of EDFA. In addition, as the cycle number increases, the accumulation of the amplified spontaneous emission (ASE) noise also deteriorated the flatness and tone-to-carrier-ratio of the multicarrier. A self-induced auto-tracking filter [22] or EDFA with flatter gain spectrum is an option to improve multicarrier quality. In order to analyze the frequency linearity and frequency interval of the multicarrier optical signal, we performed linear fitting on the frequency values of 49 subcarriers as shown in Fig. 6. The  $R^2$  value of the linear fitting is 0.99998 and the frequency interval is approximately 10.014 GHz, which is equal to the RF signal frequency. The experimental results are consistent with the theoretical analysis and proved the feasibility of the scheme of self-oscillation multicarrier light source based on RFSL.

#### IV. CONCLUSION

We presented and demonstrated a novel scheme of self-oscillation multicarrier light source. The generation of driven RF signal and multicarrier optical signal was successfully realized by optical-electrical-optical self-oscillation, which greatly reduced the system cost and was good to the miniaturization of the system. Meanwhile, the RF signal generated by self-oscillation had lower phase noise. In the experiment, we successfully obtained a single-mode oscillation RF signal and the phase noise of the RF signal was  $-85.10$  dBc/Hz at 10 kHz offset frequency. A flat multicarrier optical signal from 1550.59 nm to 1554.44 nm with the power fluctuation of 3 dB was also generated. The total number of subcarriers was 49 and the frequency interval between two adjacent subcarriers was approximately 10.014 GHz, which was equal to the RF signal frequency. It should be pointed out that the multicarrier light source proposed in this paper lacks tunability due to the fixed bandpass of the electrical filter. We are trying to use tunable electrical filter or design microwave photonic filter to improve multicarrier tunability. Further research is in progress.

#### REFERENCES

[1] Y. Wei *et al.*, "SSB single carrier and multicarrier in C-Band FSO transmission with KK receiver," *J. Lightw. Technol.*, vol. 38, no. 18, pp. 5000–5007, 2020.

[2] P. Li *et al.*, "Photonic generation of multicarrier phase-coded microwave signals utilizing polarization manipulation," *IEEE Photon. J.*, vol. 10, no. 5, Sep. 2018, Art. no. 5501708.

[3] X. Wang *et al.*, "Generation of coherent multicarrier signals for the measurement of multicarrier multipactor," *IEEE Trans. Instrum. Meas.*, vol. 66, no. 12, pp. 3357–3363, Dec. 2017.

[4] Z. Jiang, C. Huang, D. E. Leaird, and A. M. Weiner, "Optical arbitrary waveform processing of more than 100 spectral comb lines," *Nat. Photon.*, vol. 1, no. 8, pp. 463–467, Aug. 2007.

[5] V. R. Supradeepa *et al.*, "Comb-based radiofrequency photonic filters with rapid tunability and high selectivity," *Nat. Photon.*, vol. 6, no. 3, pp. 186–194, Mar. 2012.

[6] G. Gavioli *et al.*, "Ultra-Narrow-Spacing 10-Channel 1.12 Tb/s D-WDM long-haul transmission over uncompensated SMF and NZDSF," *IEEE Photon. Technol. Lett.*, vol. 22, no. 19, pp. 1419–1421, Oct. 2010.

[7] F. A. Gutierrez, P. Perry, E. P. Martin, A. D. Ellis, F. Smyth, and L. P. Barry, "All-analogue real-time broadband filter bank multicarrier optical communications system," *J. Lightw. Technol.*, vol. 33, no. 24, pp. 5073–5083, Dec. 2015.

[8] T. M. Fortier *et al.*, "Generation of ultrastable microwaves via optical frequency division," *Nat. Photon.*, vol. 5, no. 7, pp. 425–429, Jun. 2011.

[9] F. Mihelic, D. Bacquet, J. Zemmouri, and P. Szriftgiser, "Ultrahigh resolution spectral analysis based on a Brillouin fiber laser," *Opt. Lett.*, vol. 35, no. 3, pp. 432–434, Feb. 2010.

[10] Y. Kim, J. Jin, Y. Kim, S. Hyun, and S. Kim, "A wide-range optical frequency generator based on the frequency comb of a femtosecond laser," *Opt. Exp.*, vol. 16, no. 1, pp. 258–264, Jan. 2008.

[11] S. Pan, C. Lou, and Y. Gao, "Multiwavelength erbium-doped fiber laser based on inhomogeneous loss mechanism by use of a highly nonlinear fiber and a Fabry-Perot filter," *Opt. Exp.*, vol. 14, no. 3, pp. 1113–1118, Jan. 2006.

[12] L. Shang, A. Wen, G. Lin, and Y. Gao, "A flat and broadband optical frequency comb with tunable bandwidth and frequency spacing," *Opt. Commun.*, vol. 331, pp. 262–266, Jun. 2014.

[13] G. K. M. Hasanuzzaman, A. Kanno, P. T. Dat, and S. Iezekiel, "Self-Oscillating optical frequency comb: Application to low phase noise millimeter wave generation and radio-over-fiber link," *J. Lightw. Technol.*, vol. 36, no. 19, pp. 4535–4542, Oct. 2018.

[14] G. K. M. Hasanuzzaman, H. Shams, C. C. Renaud, J. Mitchell, A. J. Seeds, and S. Iezekiel, "Tunable THz signal generation and radio-over-fiber link based on an optoelectronic oscillator-driven optical frequency comb," *J. Lightw. Technol.*, vol. 38, no. 19, pp. 5240–5247, Oct. 2020.

[15] C. Lei, H. Chen, M. Chen, Y. S., and S. Xie, "Recirculating frequency shifting based wideband optical frequency comb generation by phase coherence control," *IEEE Photon. J.*, vol. 7, no. 1, Feb. 2015, Art. no. 1300107.

[16] J. Li, H. Ma, Z. Li, and X. Zhang, "Optical frequency comb generation based on dual-polarization IQ modulator shared by two polarization-orthogonal recirculating frequency shifting loops," *IEEE Photon. J.*, vol. 9, no. 5, Oct. 2017, Art. no. 7906110.

[17] J. Zhang *et al.*, "Theoretical and experimental study on improved frequency-locked multicarrier generation by using recirculating loop based on multifrequency shifting single-sideband modulation," *IEEE Photon. J.*, vol. 4, no. 6, Dec. 2012.

[18] W. Liu, W. M., and J. Yao, "Tunable microwave and sub-terahertz generation based on frequency quadrupling using a single polarization modulator," *J. Lightw. Technol.*, vol. 31, no. 10, pp. 1636–1644, May 2013.

[19] Z. Jiang, Z. Wang, T. Xie, Q. Yuan, and C. Ge, "Dual-frequency light source with widely tunable frequency difference based on single-side-band modulator," *Opt. Commun.*, vol. 445, pp. 50–55, Mar. 2019.

[20] X. S. Yao and L. Maleki, "Optoelectronic microwave oscillator," *J. Opt. Soc. Amer. B.*, vol. 13, no. 2, pp. 1725–1735, Aug. 1996.

[21] X. S. Yao and L. Maleki, "Multiloop optoelectronic oscillator," *IEEE J. Quantum Electron.*, vol. 36, no. 1, pp. 79–84, Jan. 2000.

[22] Z. Wang *et al.*, "Broadband lightwave synthesized frequency sweeper using self-induced auto-tracking filter," *Opt. Exp.*, vol. 23, no. 17, pp. 22134–22140, Aug. 2015.